NANOTUBE COMPOSITE COATINGS AS STRAIN SENSORS ON GLASS FIBRES IN EPOXY COMPOSITES

Paweena Sureeyatanapas, Marek Hejda, Stephen J. Eichhorn, Robert J. Young

School of Materials, University of Manchester, Grosvenor Stress, Manchester, M1 7HS, UK
robert.young@manchester.ac.uk

ABSTRACT

The study of the interfacial properties of glass fibres in polymer composites by fragmentation is not normally carried out using Raman Spectroscopy since the glass is a Raman inactive material. However, when carboxylic acid functionalized single-walled carbon nanotubes (COOH-SWNTs) are added to the silane solution in the sizing process, it is become possible for glass materials to be mechanically studied by Raman Spectroscopy. SWNTs were incorporated as a strain sensor on the fibre surface and interacted with the glass, silane chemical, and epoxy resin. Moreover, glass fibre containing a small amount of Sm_2O_3 as one of the components can be a Luminescence active sensor in the same manner as SWNT sensor, using Fluorescence Spectroscopy. A micromechanical properties study of stress transfer at the fibre-matrix interface using Raman spectroscopy together with Fluorescence Spectroscopy, which can be set up using a Raman Spectrometer, is reported. The Sm^{3+} component was in the glass composition while SWNTs were distributed along the fibre surface by dispersing them in an amino-silane coupling agent. The point-by-point strain mapping of the fibre in single fibre fragmentation tests and the interfacial shear stress (ISS) distribution along the fibre length was determined using the Sm^{3+} and embedded SWNTs as sensors. The behaviour was found to be consistent with the classical shear-lag model. This fact clearly indicate that SWNTs and Sm^{3+} are excellent sensors for glass fibres and can be applied to other Raman inactive materials in the future.

1. INTRODUCTION

Because of high mechanical strength, good chemical resistance and compatibility with the matrices of glass fibres and good mechanical and thermal properties, excellent chemical resistance and low cure shrinkage of epoxy resins; glass fibre reinforced epoxy composites are widely studied. The properties of the composites combined with their low cost leads to the use in a number of critical applications such as in civil aircraft, jet engines, wind turbines, space structures and piping systems for offshore environments [1]. One crucial factor to control the properties of composites is the fibre-matrix interface. The modification of the interface to strengthen the chemical bonding between the fibre and the matrix using silane treatment has been applied [2]. Various methods have been used to characterize the stress transfer from the matrix to the reinforced materials and the properties of the interface to understand the behaviour of the composites. These micromechanical tests are the pull-out test [3] and fragmentation test [4, 5]. Recently the Raman scattering technique has been implemented to analyse the micromechanics of the system. This can only be achieved if a strong Raman spectrum is obtained from the reinforcement and if a matrix is transparent.

However, glass fibres does not provide a well-defined Raman signal, incorporating a Raman active material has been successfully applied to follow the fibre deformation and micromechanical behaviour. This process has effectively solved the problem of the study of glass fibre deformation behaviour using Raman technique. The first successful micromechanical study to follow interfacial stress transfer of a glass-fibre/epoxy composite system using Raman spectroscopy was carried out by Young et al [5]. A diacetylene-urethane copolymer as a strain sensor was coated on the fibres to map the

strain distribution along the fibre during fragmentation test. Single walled carbon nanotubes (SWNTs) distributed within the epoxy matrix to sense the stress around the glass fibre has also been widely studied [6, 7]. A recent study on application of a sizing containing SWNTs onto the surfaces of glass fibre to follow the deformation of glass fibres in polypropylene composites were undertaken by Wagner et al [8]. Meanwhile fluorescence spectrum of Cr^{3+} doped sapphire [9] has been used to follow the stress under compression so as that used in a single alumina fibre [10] in fragmentation analysis using luminescence process. Moreover, the same technique has been applied to dope the glass fibre with Er^{3+} to follow the residual stresses [11]. A recent study by Eichhorn et al [12] on the use of samarium fluoride (SmF_3) to follow the stress state in glass has also been successful.

In this paper, the possibility to direct point to point strain mapping along the Sm^{3+} doped E-glass fibre embedded in the epoxy matrix by using sizing SWNTs as a sensor on the glass fibre surface to monitor the deformation and behaviour have been investigated. Furthermore Sm^{3+} has also been used as an inner sensor to compare the efficiency of SWNTs as a sensor on the fibre surface. It also includes the methodology of Sm^{3+} doped glass fibre production and a preparation of well distribution of SWNTs along a glass fibre. The aims was to study the micromechanical behaviour of the interfaces of glass-fibre/epoxy composites using a cross check sensors from Sm^{3+} doped in-situ E-glass and SWNTs at the interface. Furthermore, this particular technique was also practical to the determination of the interfacial shear stress (ISS) of the fibres.

2. EXPERIMENTS

2.1 Materials

In this study, glass rods were firstly synthesized in 1500 ^{o}C using the composition of 55% SiO_2, 6.5% Al_2O_3, 12.9% CaO, 0.5% Na_2O, 3.0% MgO, 9.9% B_2O_3, 0.3%SO_3 and 0.8% Sm_2O_3. Then the rods were hot stretched under a gas flame to produce glass fibres of which the diameter ranges between 40 – 60 microns. The Sm^{3+} ions were presented in the sufficient amount for its luminescence spectrum to be detected. Carbon nanotubes used in this work were single-walled nanotubes produced by electric arc-discharge then functionalized by carboxylic acid functional group, purchased from Sigma-Aldrich Co., Ltd. The epoxy resin matrix was a mixture of Araldite resin LY5052 (a butan-1,4 diol diglycidyl ether resin) and Aradur hardener HY5052 (a isophonorone diamine) supplied by Vantico, Polymer Specialties, UK. The mixing ratio was 100 parts of LY5052 to 38 parts of HY5052. The silane coupling agent used was an amino-silane, 3-aminopropyl-triehtoxysilane, supplied by Avocado Research Chemicals, UK

2.2 Sample preparation

0.1% SWNTs in ethanol solution were firstly sonicated for 2 hours before 1.5% silane chemical was added. The glass fibres were then treated in the mixture solution for 10 – 15 minutes before drying or condensation in the oven. Then the fibres were coated with ethanol/epoxy mixture and hot cure in 120 ^{o}C for 2 hours.

The fibres were then prepared for the mechanical testing called the ‘single fibre deformation test’ and ‘fragmentation test’. In the deformation test, 50 mm gauge length fibre was mounted onto a cardboard and fixed to a single fibre deformation rig. The cardboard was subsequently cut leaving the stand alone fibre on both sides of the rig. It

was then ready for the test. Meanwhile, in the fragmentation test, a 20 mm sized fibre was embedded in the dumbbell shape epoxy matrix specimen and cold cured at room temperature at least for 7 days before the experiment.

2.3 Fibre characterization

Forty single fibres of 50 mm gauge length were firstly mechanical property tested by deforming in axial tensile using an Instron 1121 tensile testing machine. The machine was set up with a 10 N load cell using a cross-head speed of 0.5 mm per minute under controlled temperature (23±1 °C) and humidity (50±5%). Stress-strain curves were then plotted to determine the fibre Young modulus (E).

Scanning electron microscope (JEOL 6300 SEM) was used to characterize the SWNTs-sizing on glass fibre surface. Gold particle was slightly coated for 10 seconds to create a conductive thin layer and minimize the thick coating layer which could interrupt the sized SWNT observation. The machine was operated at 5 kV to minimize charging.

2.4 Raman Spectroscopy

Raman Spectroscopy was used to characterize the basic spectrum of SWNTs and Sm^{3+}. Raman spectra were collected using Renishaw 1000 Raman Spectrometer equipped with an Olympus BH-2 microscope. A 50x long working distance objective lens were used. HeNe laser was used for examination of SWNTs for Raman scattering process whereas argon laser were used for that of Sm^{3+} for luminescence process. The laser beam was focused in the middle of fibre for Sm^{3+} and focused on the surface where there were slight SWNTs attached to the glass surface. The spectra of SWNTs were recorded using 15 seconds and 2 accumulations with 10% maximum intensity of laser power for specific area of interest, whereas those of Sm^{3+} were recorded using 10 seconds and 3 accumulations with 10% laser power. The full wave number range of SWNTs was 100 – 3000 cm^{-1} while that of Sm^{3+} was 550 – 700 nm.

3. RESULT AND DISCUSSION

3.1 Fibre characterization

The fibres micromechanical tested by Instron 1121 machine were found to have a mean Young's modulus of 76 GPa which is about the same value as the commercial E-glass fibre. Therefore, having Sm_2O_3 was not significant affect to the mechanical properties.

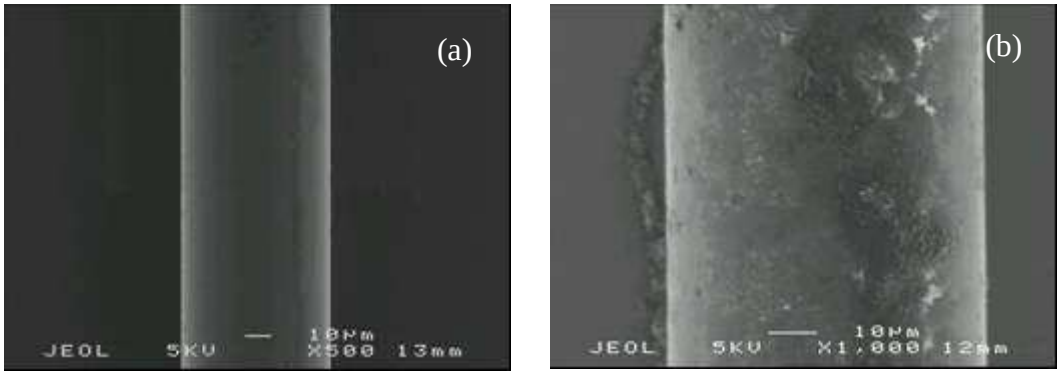

Figure 1: SEM images of glass fibre before sizing (a) and after SWNTs/silane sizing (b)

Figure 1 showed SEM images compared between glass fibres before the SWNTs/silane sizing and after the sizing. As it can be clearly seen that the roughness of the surface increased and there were some lumps of aggregated SWNTs on the fibre surface after the sizing process. This will increase the adhesion properties of glass fibre bonding to the resin [2].

SWNT as a good electrical and high mechanical strength has their unique Raman band spectrum. It gives a very strong, well-defined resonance Raman spectra which consists of 4 main bands; a radial breathing mode at 100-400 cm^{-1} (RBM), a defect induced mode at 1300-1500 cm^{-1} (D band), a tangential mode at 1500-1600 cm^{-1} (G band), and an overtone of D band at 2500-2700 cm^{-1} (G'band). It has been known that the G'band shifts significantly from its original position during deformation. It shifts to lower wave number when SWNTs are under tension and to higher number when SWNTs are under compression [6, 7]. Deformation of SWNTs can therefore be followed by monitoring the Raman G'band position changes. The full spectrum of SWNTs was shown in Figure 2a The G'band was obtained in the range of 2400 – 2800 cm^{-1}.

Sm^{3+} also has a unique luminescence spectrum. The full spectrum of Sm^{3+} doped glass fibre was shown in Figure 2b. Although there are several sharp peaks in this region; the most intense peak was chosen to follow the local strain in this study. The other peaks were found to shift as well but they were not as significant as the peak at 648 nm [11,12]. This band was then focused in the range of 640 – 660 nm.

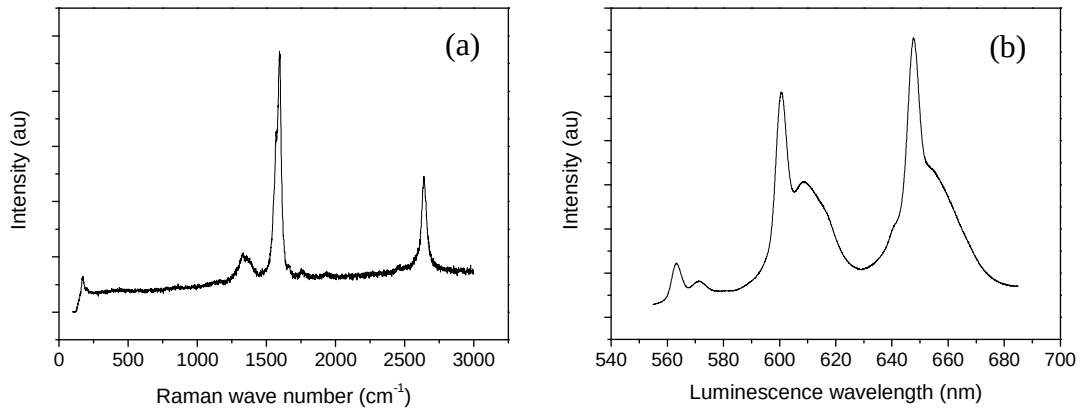

Figure 2: Full range of SWNTs band (a) and Sm^{3+} band (b)

Both Raman spectra of SWNTs and luminescence spectra of Sm^{3+} were very intense compared to those of glass fibre and epoxy resin in the same region (not shown here). Therefore, there was barely effect of spectra from glass fibre and epoxy interfering in the experiment.

3.2 Fibre deformation

The aim of a single fibre deformation test was to find the relationship of the band position shift of SWNTs and Sm^{3+} to % fibre strain. A calibration curve obtained from a single fibre deformation was then used to convert the band position to % fibre strain for a fragmentation test. In the fragmentation test, the fibre in the composites were axial tensile strained by increasing axial load until the fibre break into fragments. The point

by point strain mapping along the fibre from one end to the other was carried out through each step of strain level.

3.2.1 Single fibre deformation test

In a single fibre deformation test, a small level of strain was applied at each step until the fibre break. In each step, a Raman G'band spectrum of SWNTs at 2640 cm^{-1} and a luminescence band spectrum of Sm^{3+} at 648 nm were collected. The shifted positions of these bands are shown in Figure 3a and 3b respectively. As they can be seen that after the strain was applied to the fibre the band position of the strain sensitive materials shifted to lower wave number as predicted [5-12]. The band position shifts were finally plotted versus % fibre strain as in Figure 4. The average Raman band shift rate of SWNTs sizing on glass fibre was -23.25 cm^{-1} while luminescence shift rate of Sm^{3+} doped glass fibre was -0.079 nm/%strain or -1.89 cm^{-1}/%strain.

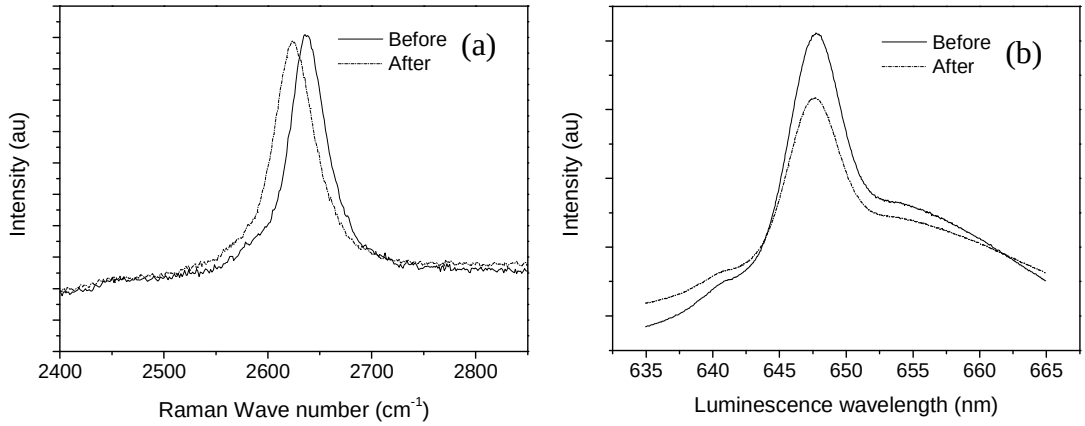

Figure 3: Raman band position shift before and after the applied strain of SWNTs (a) and luminescence position shift of Sm^{3+} (b)

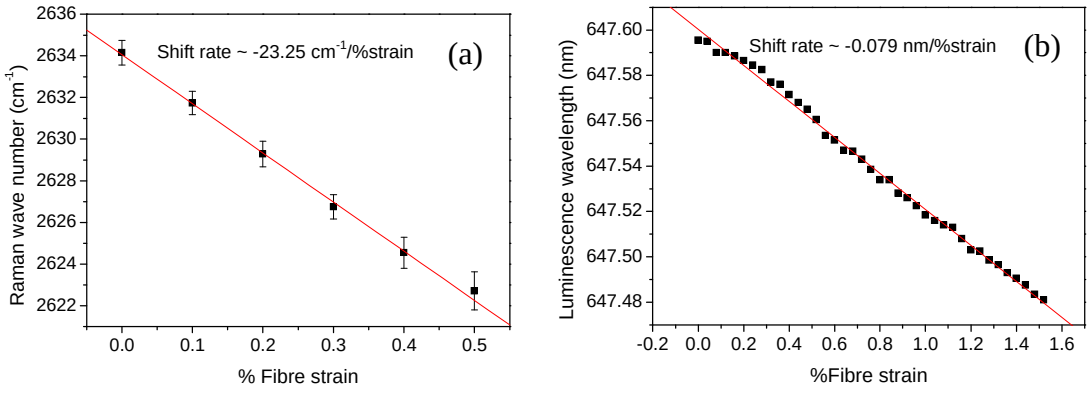

Figure 4: Raman shift rate of SWNTs (a) and luminescence shift rate of Sm^{3+} (b)

3.2.2 Fragmentation test

In the fragmentation test, a specimen was placed in a minimat deformation rig and the experiment was carried out under Raman Spectroscopy. Firstly matrix strain measured by strain gage was increased from 0% to 0.4% and 0.8%. In each step, the sizied SWNTs along the fibre surface were focused along the fibre from one end to the other

and data collected by HeNe laser. These SWNTs were assumed to have a perfect bond to the fibre and to the matrix so that it can represent the fibre strain in the composites. The experimental data were finally plotted and compared to classical shear-lag model or Cox's model. The model assumes that the system is in elastic region and there is a perfect bond between the fibre and the matrix [13]. The equations used to calculate fibre strain (ε_f) and interfacial shear stress (ISS or τ) are shown below;

$$\varepsilon_f = \varepsilon_m \left[1 - \frac{\cosh \beta \left(\frac{l}{2} - x \right)}{\cosh \beta \frac{l}{2}} \right] \quad (1)$$

$$\tau = E_f e_m \left[\frac{G_m}{2E_f \ln\left(\frac{R}{r}\right)} \right]^{\frac{1}{2}} \left[\frac{\sinh \beta \left(\frac{l}{2} - x \right)}{\cosh \beta \frac{l}{2}} \right] \quad (2)$$

Where $\beta = \left[\frac{2G_m}{E_f r^2 \ln \frac{R}{r}} \right]^{\frac{1}{2}}$, $G_m = \frac{E_m}{2(1+\nu)}$, x = distance along the fibre, ε_m = matrix strain, r = fibre radius, R/r = fitting parameter, ν = Poisson ratio , E = Young's modulus (subscript m for matrix and f for fibre)

The strain mapping along the length of the glass fibre embedded in the epoxy matrix is shown in Figure 5a. Only SWNTs that distributed along the fibre were acquired in this sample using HeNe laser. It can be seen that the sized SWNTs were well distributed along the fibre since any points along the fibre could be mapped. It was found that at unstrained state (matrix strain = 0%), the G'band position of SWNTs showed less than 0.05% scatter around 0% fibre strain. This may due to the variation of aggregation and contraction state of individual SWNTs bonded to the fibre and epoxy. Once the matrix was deformed to higher strain level, the fibre strain increased from 0% at one end to the constant value approach to the matrix strain value in the middle region and decreased to 0% at the other end [5, 12]. This corresponds to the prediction of shear-lag theory [13]. Further matrix strain applied caused the fibre to fracture into 4 fragments. At the fibre broken points, G'band of SWNTs position showed unstrained stage as those at the fibre ends. The positions around the break points also behave as individual fibre end points. This indicated that there is no stress transfer across the fibre ends and fibre broken points.

Analysis of interfacial shear stress (ISS or τ) was also important to the study of composite properties. The ISS along the fibre length was determined using the force balance equation [12]. Figure 5b shows the variation of ISS with distance along the fibre from the same sample. At the fibre broken points and at the fibre ends, the ISS were at the maximum compared to those at the middle area of the fracture where they were approached to zero. The maximum value of ISS found was no more than 20 MPa, less than the yield stress of the resin matrix (40 MPa). This indicated that the matrix was

still undergoing elastic deformation and stress transfer at the interface was therefore followed elastic shear-lag theory [13].

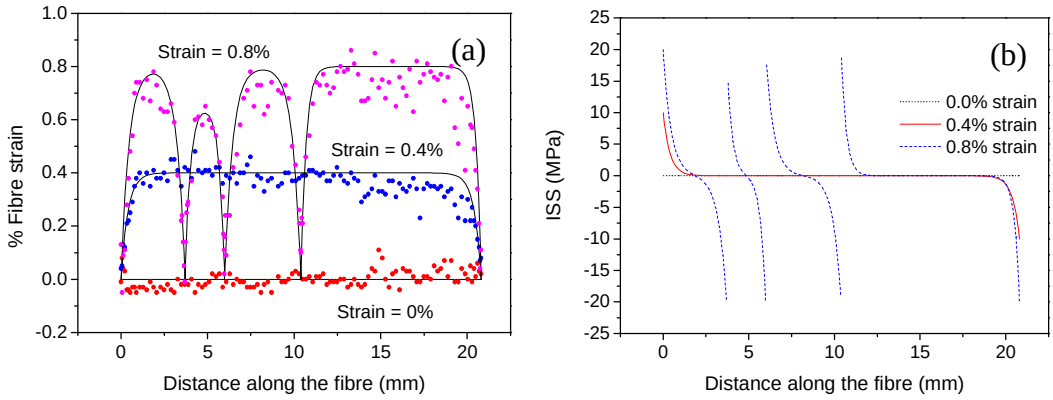

Figure 5: Strain mapping along the length of the fibre collected from sized SWNTs as a strain sensor

However, there has been a suspicious of SWNTs interfering to the interfacial properties of the composites. Therefore, in the next step, the two strain sensors will be compared and tested from the same sample at the same time. This experiment was aim to prove whether the sized SWNTs at the fibre interface had effect to the interfacial properties of the composites and whether it was a sufficient sensor for this application. Sm^{3+} which was doped with E-glass fibre previously in the production process was focussed and scanned from one fibre end to the other along the fibre length using Argon laser and followed by SWNTs scanning in the same way using HeNe laser. Then the load was increased in the step of 0%, 0.4%, 0.7% and 1.0% respectively. The experimental data of strain distribution along the fibre from SWNTs using Raman scattering process from HeNe laser were plotted compared with the data from Sm^{3+} using luminescence process from Argon laser. Then they were fitted to shear-lag model.

The result of this experiment is shown in Figure 6a. The trend of strain mapping data using SWNTs in each strain level was the same as the result in Figure 5a which showed the increasing of fibre strain along with the increasing of matrix strain from both fibre ends to the middle area of the fibre. And at the high strain level of 1.0% where the fibre fractured, each fragment behaved as an individual fibre. Furthermore, the experimental data were well fitted with the theory of fibre strain distribution in the composites by the shear-lag model. Therefore, it can be concluded that SWNTs can represent the strain in the fibre. In the mean time, at matrix strain level of 0.7% and 1.0%, the experimental data collected from Sm^{3+} in Figure 6b were surprisingly well fitted with the model and the strain in fibre detected showed the same behaviour as that obtained from SWNTs. Comparing between SWNTs and Sm^{3+} data at the same strain level of 0.7% matrix strain as in Figure 6c, it can be observed that the trend of fibre strain sensed from Sm^{3+} was slightly higher than that from SWNTs. More obvious difference can be observed at 1.0% matrix strain where the fibre broke into several fragments as in Figure 6d. The reason might be because the experiment was carried out by collecting the data from Sm^{3+} earlier than SWNTs in each strain level so the lag time of data collection of SWNTs might cause the stress relaxation in the system. As this matter, in order to fit the data to the model, the different matrix strain was estimated for the data from Sm^{3+} and

SWNTs at 1.0% matrix strain. Moreover, it was found that the fibre in the 4th fragment, which had the longest length among all, further broke into 2 smaller fragments when the specimen was under stress for a long period of time as could be detected only from the data obtained from SWNTs, not that from Sm^{3+}. This can lead to the prediction of the future fragment if the specimen were loaded more or being held for a longer time. It was finally brought about the conclusion of SWNT efficiency as a sufficient strain sensor for glass materials to be tested by Raman spectroscopy without the fundamental effect of the interface properties.

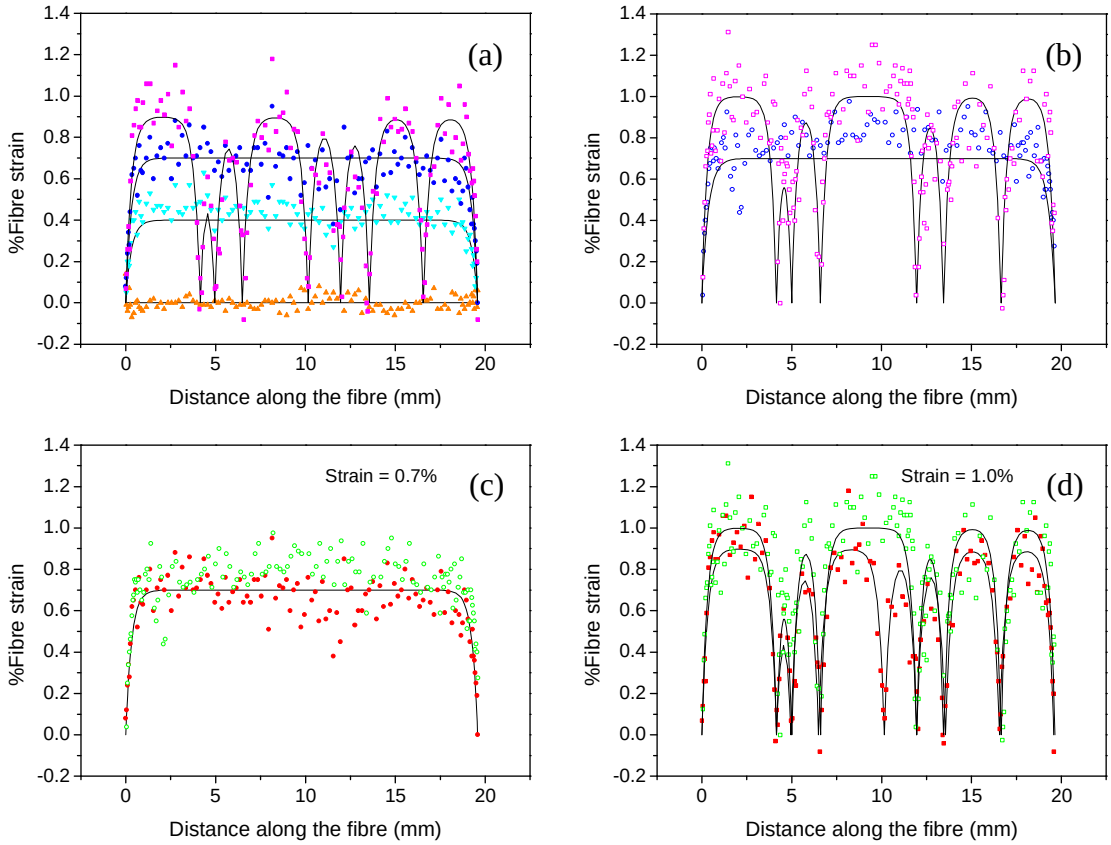

Figure 6: Strain mapping analysis of Sm^{3+} doped E-glass fibre using SWNTs as a strain sensor (a) and using Sm^{3+} as a strain sensor (b). Compare between SWNTs and Sm^{3+} as sensors at 0.7% matrix strain (c) and at 1.0% matrix strain (d). Closed circle and closed square are the data from SWNTs while opened circle and opened square are the data from Sm^{3+}

ISS along the fibre length was also determined again using the experimental data from the same sample as in Figure 6. Figure 7a and 7b show the variation of ISS at the 0.7% and 1.0% matrix strain respectively obtained from Sm^{3+} while Figure 7c shows the variation of ISS at the 0%, 0.4%, and 0.7% matrix strain and Figure 7d at 1.0% matrix strain obtained from SWNTs. Same trend as the previous sample was observed with the maximum value of ISS between 20-25 MPa for both ISS estimated by SWNTs and Sm^{3+}. At 1.0% strain, the ISS mapping showed almost straight line for the small fragment and similar line but with the flat area in the middle for the bigger fragment length. It was also found that there was an extra ISS line existed from further broken fragment in the case of data sensed by SWNTs as the reason explained previously.

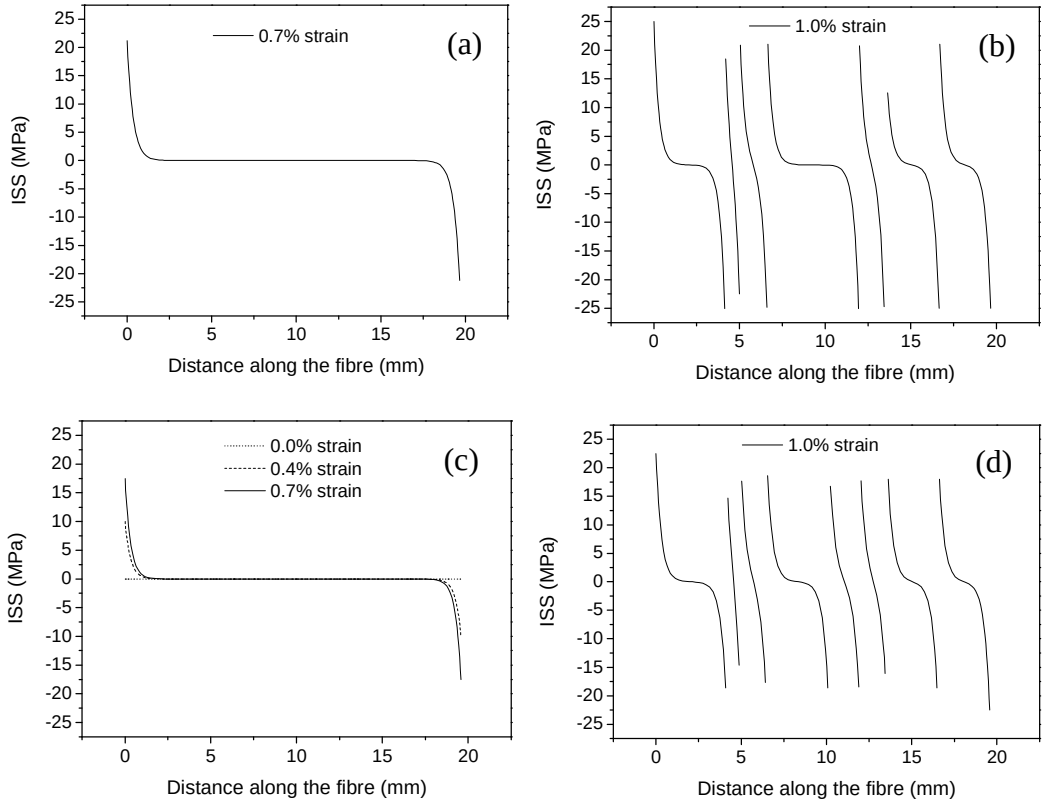

Figure 7: Interfacial Shear Strength (ISS) of the fibre shown in Figure 6 at 0.7% matrix strain (a) and 1.0% matrix strain (b) fitting by the data obtained from Sm^{3+}. ISS fitting of the fibre in Figure 6 at 0.0%, 0.4% and 0.7% matrix strain (c) and 1.0% matrix strain (d) by data obtained from SWNTs.

4. CONCLUSION

This paper has demonstrated the possibility to employ single-walled carbon nanotubes (SWNTs) as a strain sensor for glass fibres through the use of Raman spectroscopy. Using this technique to follow the interface of glass fibre in epoxy composites has been a difficult problem. As the SWNTs sizing which thoroughly distributed along the fibre length was at the interface between the glass fibre and the epoxy-resin matrix, it was possible to use Raman spectroscopy to monitor the strain at the fibre-matrix interface during deformation. The results were well fitted to the classical shear lag model. To merge the recently successful of using Sm^{3+} as another strain sensor to prove the efficiency of SWNTs as a sensor, this particular work of producing special Sm^{3+} doped E-glass fibre with sized SWNTs and testing was undertaken. The variation of the strain in the fibre along the fibre length was shown to follow the classical shear-lag model as well. Consequently, the data measurement by SWNTs from Raman spectroscopy and that by Sm^{3+} from luminescence were in agreement. Doubt in any using SWNTs as a strain sensor whether or not to affect the interface properties at the interface has been clarified. However, there will be plenty of scope for improvement for better efficiency and for further applications.

ACKNOWLEDGEMENTS

The work presented in this paper has been funded by the Government of Thailand and further supported by the EPSRC in the form of a research grant (EP/C002164/1). The authors would kindly like to acknowledge the assistance of all the technicians from the School of Materials.

REFERENCES

1- Phillips, L.N., "Design with Advanced Composite Material", *The Design Council*, 1989: 1-32, 69-117
2- Khazanov, V.E., Kolesov, Y.I., and Trofimov, N.N., "Glass Fibre", in *Fibre Science and Technology*, 1995; Chapman & Hall: London: 15-212.
3- Miller B., Muri P., Rebenfeld L., "A microbond method for determination of the shear-strength of a fibre-resin interface", *Composite Science Technology*, 1987; 28:17-32
4- Kelly A., Tyson W.R., "Tensile properties of fibre-reinforced metals - copper/tungsten and copper/molybdenum", *Journal of the Mechanics and Physics of Solids*, 1965:13;329-50
5- Young, R.J., et al., "Fragmentation analysis of glass fibres in model composites through the use of Raman spectroscopy",*Composites Part A: Applied Science and Manufacturing*, 2001; **32**(2): 253-69
6- Wagner, H.D., et al., "Stress fields around defects and fibres in a polymer using carbon nanotubes as sensors", *Applied Physics Letters*, 2001; 72(12): 1748-1750
7- Dharap, P., et al., Nanotube film based on single-wall carbon nanotubes for strain sensing", *Nanotechnology*, 2004; 15: 379-82
8- Barber, A.H., et al., "Characterization of E-glass-polypropylene interfaces using carbon nanotubes as strain sensors", *Composites Science and Technology*, 2004; 64(13-14): 1915-19
9- He, J., Clarke, D.R., "Determination of the piezospectroscopic coefficients for chromium-doped sapphire", *Journal of the American Ceramic Society*, 1995; 78: 1347-53
10- Yallee, R.B., Young, R.J., "Micromechanics of fibre fragmentation in model epoxy composites reinforced with alpha-alumina fibres", *Composites: Part A*, 1998; 29A: 1353-62
11- Leto, A., Pezzotti, G., "Probing nanoscale stress fields in Er3+ doped optical fibres using their native luminescence", *Journal of Physics: Condensed Matter*, 2004; 16: 4907-20
12- Eichhorn, S.J., et al., "Deformation micromechanics of model glass fibre composites", *Composites Science and Technology*, 2008; 68: 848-53
13- Cox, H.L., "The elasticity and strength of paper and other fibrous materials", *British Journal of Applied Physics*, 1952; 3: 72-79